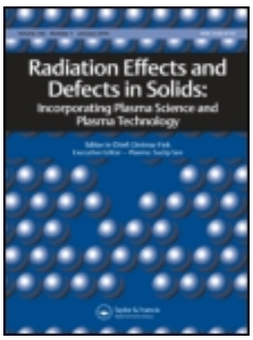

Radiation Effects and Defects in Solids

ISSN: 1042-0150 (Print) 1029-4953 (Online) Journal homepage: http://www.tandfonline.com/loi/grad20

Experimental layout for the realization of an X-ray plasma source driven by a Nd:YAG laser for biological and medical applications

L. Palladino , T. Limongi , G. Gualtieri , R. Gimenez De Lorenzo & P. Zuppella

To cite this article: L. Palladino , T. Limongi , G. Gualtieri , R. Gimenez De Lorenzo & P. Zuppella (2008) Experimental layout for the realization of an X-ray plasma source driven by a Nd:YAG laser for biological and medical applications, Radiation Effects and Defects in Solids, 163:4-6, 505-512, DOI: 10.1080/10420150701780615

To link to this article: http://dx.doi.org/10.1080/10420150701780615

Radiation Effects & Defects in Solids
Vol. 163, Nos. 4–6, April–June 2008, 505–512

Taylor & Francis
Taylor & Francis Group

Experimental layout for the realization of an X-ray plasma source driven by a Nd:YAG laser for biological and medical applications

L. Palladino[a,c]*, T. Limongi[a,b], G. Gualtieri[b], R. Gimenez De Lorenzo[a] and P. Zuppella[a]

[a]Department of Physics, L'Aquila University, L'Aquila, Italy; [b]Department of Science and Biomedical Technology L'Aquila University, L'Aquila, Italy; [c]Laboratorio Nazionale del Gran Sasso, INFN Instituto Nazionale di Fisica Nucleare, Assergi (AQ)

(*Received 13 February 2007; in final form 4 September 2007*)

In this paper, an experimental set-up for the X-ray production (≈70 eV–25 keV energy range) by a plasma, obtained focalizing a high-power Nd:YAG laser beam on a specific target, is presented. The measures of the characteristics of a custom Nd:YAG high-power laser beam (maximum of 8 J at 1064 nm, 5 ns pulse duration) and a new disposition of the target–lens system in the interaction chamber are discussed. The aim of this research is the use of the plasma resulting by the focalization of the laser beam, which will be used as a soft X-ray source or an electron source instead of the hot filament of the standard mammographic X-ray tubes.

Keywords: X-ray; plasma source; electron beams generation

1. Introduction

Different applications of soft X-rays (≈70 eV–2 keV) and of hard X-rays (≈3–25 keV) in biological (*1*), in radiobiological (*2*) and in medical imaging field (*3*), have encouraged the development of the X-ray sources based on the production of plasma.

In this work, the project and realization of a non-traditional X-ray source with energy ranging from about 70 eV to about 20–25 keV (LASEX an INFN experiment) are proposed.

The emission of X-rays is due to a plasma obtained focalizing a high power Nd:YAG laser beam on different targets (Al, Cu, Y or mylar).

Soft X-rays, 70 eV–2 keV, are produced by the dynamic expansion of the plasma, while X-rays in an higher energy region (about 25 keV) are produced by the accelerated electrons of the plasma in a high-voltage potential incident on a target (Mo, Ti, W) for bremmsthralung effects. So, with this experimental set-up, a plasma produced by the focalization of a laser beam can be used independently as a source of electrons or of X-ray photons.

*Corresponding author. Email: libero.palladino@fastwebnet.it

ISSN 1042-0150 print/ISSN 1029-4953 online

DOI: 10.1080/10420150701780615
http://www.informaworld.com

This source is characterized by an instantaneous spectral high brightness, by a punctiform dimension (some tens microns, focal laser spot) and by a pulse temporal structure with the same duration of the laser in the whole spectral region.

A new concept of a plasma source interaction chamber is described; the target is not centered in the vacuum chamber, thus allowing a more flexible use of the X-ray beam in different applications.

This apparatus is under construction in the X-ray Biophysics Laboratory, Physics Department of Aquila University.

2. Experimental layout

2.1. *Nd:YAG laser system*

In Figure 1, the layout of the Nd:YAG high-power laser system (by Quanta System) used for plasma production is shown. It is composed of an oscillator [Nd:YAG rod (rod no. 1 in Figure 1)], a pre-amplifier [Nd–glass rod (rod no. 2 in Figure 1)] and two amplifiers [two Nd–glass rods (rod no. 3 and rod no. 4 in Figure 1)]. The output energies measured at the end of each rod and the other characteristics of the laser, as the repetition rate, are resumed in Table 1. With this configuration, the energy laser beam and then the power density (W/cm^2) on the target can be modulated. The power density is fundamental to determine the plasma temperature, the X-ray

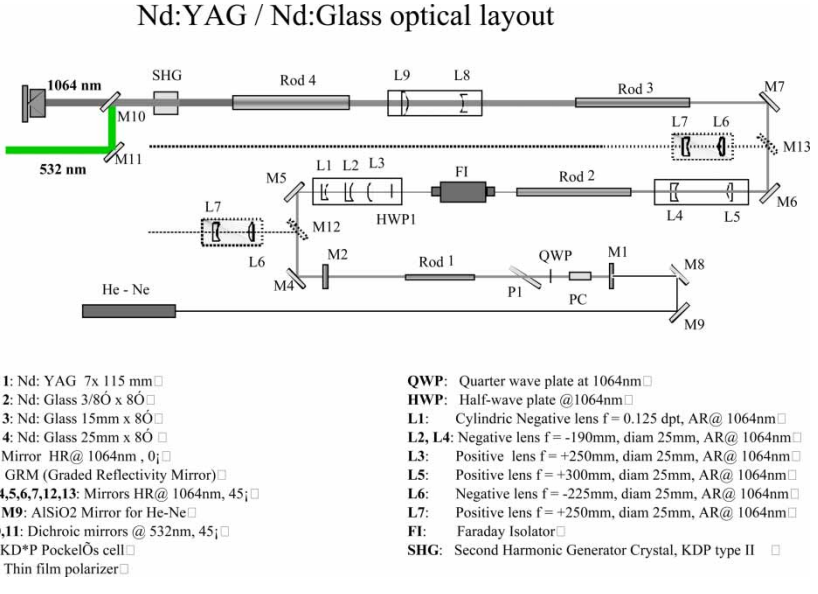

Figure 1. Nd:YAG/glass system with the fundamental components described in the legend and reported in the text.

Table 1. Nd:YAG/Nd glass characteristics.

Laser part	Energy (at 1064 nm)	Energy (at 532 nm)	Beam diameter (mm)	Repetition rate
Oscillator	240 mJ	18 mJ	7.0	1 pulse/s
+ pre-Ampl	1.5 J	380 mJ	9.5	1 pulse/min
+ Ampl No. 1	5 J	2 J	15	1 pulse/min
+ Ampl No. 2	8 J	4 J	25	1 pulse/min

emission and plasma ionization. The photon frequency of the output beam (IR at 1064 nm) can be doubled (green at 532 nm) by a second Harmonic Generator (SHG in Figure 1). The laser is protected from back-reflections of the laser beam on the target by a Faraday isolator (FI in Figure 1). The laser pulse duration is 5 ns and the measured divergence is 0.8–0.9 mrad about four times the limited diffraction. In Figures 2a and b, the pattern and densitometry profile of the laser beam in the output of Ampl 1 (Ø15 mm, 5 J at 1064 nm) is shown, and in Figures 2c and d, the pattern and densitometry profile of the laser beam in the output of Ampl 2 (Ø25 mm, 8 J at 1064 nm) is reported.

The measures of the dimensions of the focalization spots have been executed using an aspherical triplet lens, 12 cm focal length and 4 cm diameter, to reduce the geometrical aberrations.

The laser beam, at low energy pulses (about 250 mJ at 1064 nm), was focalized on a copper target, the dimension of the spot is about 80 μm, as we can see in the transmission electron microscope (TEM) image of the crater shown in Figure 3, corresponding at a power density of $\approx 10^{12}$ W/cm^2. More accurate measurements of the spot dimension will be executed using a pinhole camera.

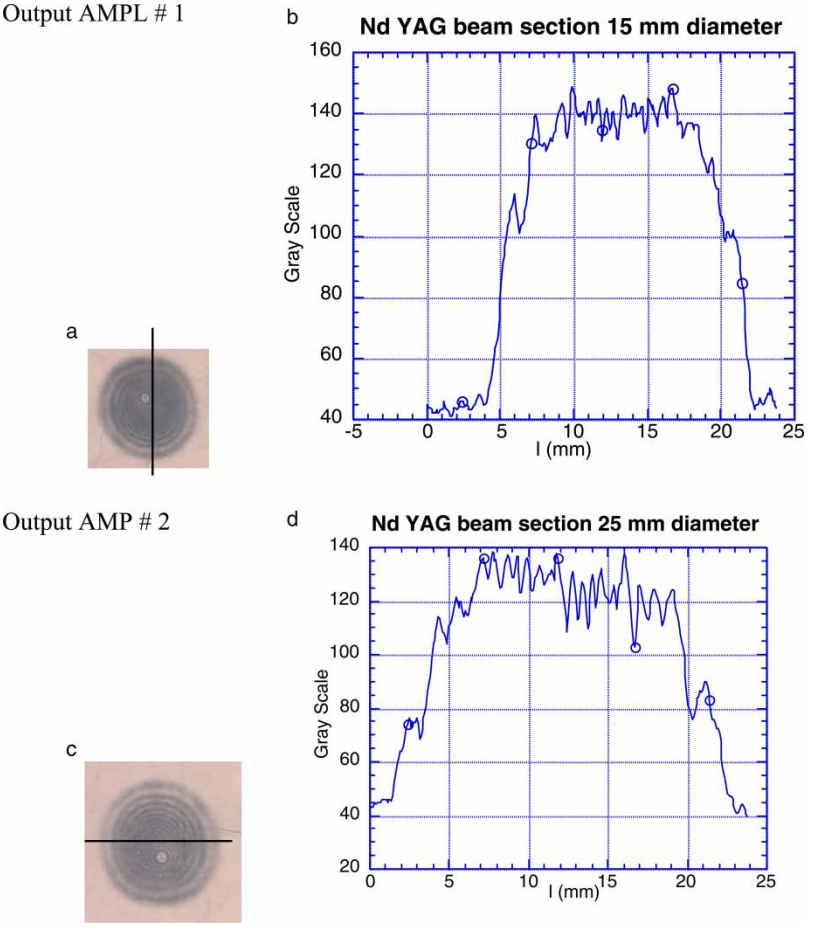

Figure 2. (a) The pattern and (b) densitometry profile of the laser beam in the output of Ampl No. 1 (Ø15 mm, 5 J at 1064 nm); (c) the pattern and (d) densitometry profile of the laser beam in the output of Ampl No. 2 (Ø25 mm, 8 J at 1064 nm).

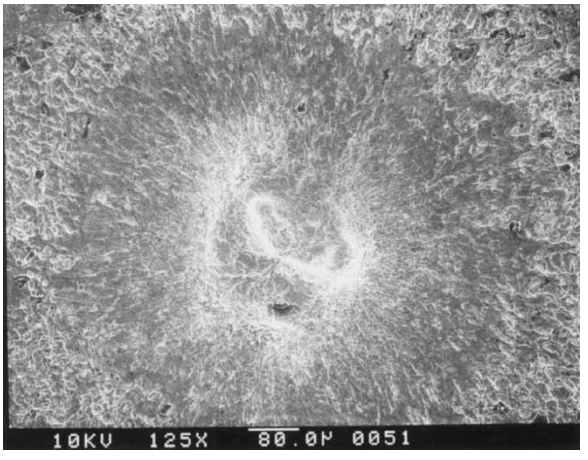

Figure 3. The transmission electron microscopic image of the crater produced by focalization of the laser beam, at low energy pulses (about 250 mJ at 1064 nm) on a copper target. The dimension of the spot is about 80 µm.

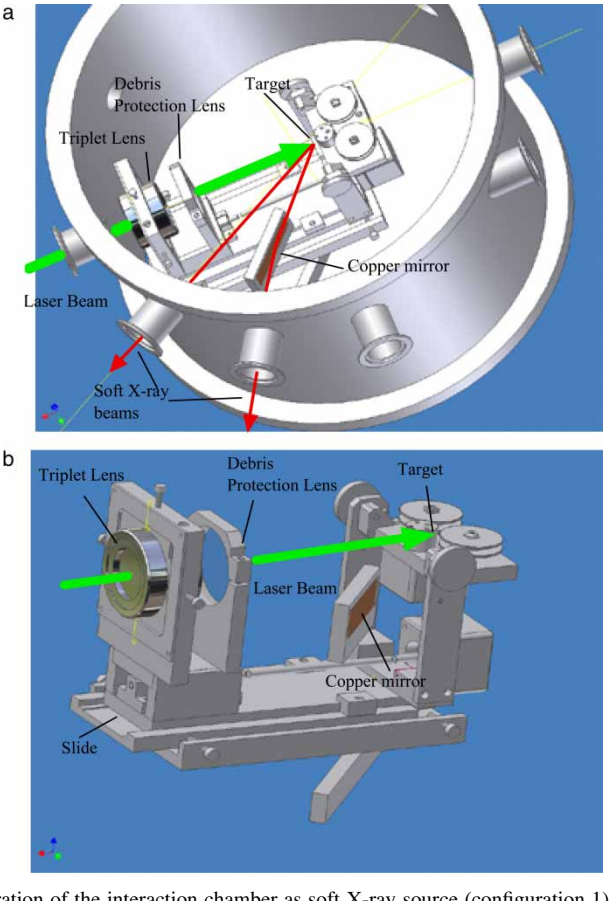

Figure 4. (a) Configuration of the interaction chamber as soft X-ray source (configuration 1). The diameter is 40 cm and can work at $p = 10^{-3}$ Torr. (b) The mechanical slide movement of the lens–target system is shown.

2.2. *The interaction chamber*

In the soft X-ray energy region, the beams are produced by dynamic expansion of the plasma and the relative configuration of the interaction chamber (configuration 1) is shown in Figure 4a. The laser beam is focalized by an aspherical triplet lens on a target and the plasma and X-ray photons are emitted in 2π Sr solid angle in the opposite direction of the laser beam. The lens is protected from the debris, produced during the ablation of the target material, by a thin circular glass window. The position of the lens with respect to the target and the renewal of the target, after every ablation, are controlled by computer. It is introduced by a new disposition of the target–lens system in the interaction chamber. In particular, it is possible to place the target in different positions with respect to the centre of the vacuum chamber. In Figure 4b, the mechanical slide of the movement of the lens–target system is shown; a mirror or a crystal is used for selecting the X-ray beams' energy intervals. As shown in Figure 5, the geometrical relation from φ angle (formed by laser beam direction and X-ray beam direction), θ angle (grazing angle to surface of the mirror or the crystal), l (CS distance in Figure 5) and h (CT distance in Figure 5) is

$$l = h\frac{\sin(\varphi - 2\theta)}{\sin(2\theta)}.$$

The X-rays ranging from ≈200 eV up to ≈800 eV are used in several biomedical and X-ray microscopy applications (*1*). To select the photons in this energy region, a copper mirror at fixed grazing incidence and helium gas at 1 atm are used. In fact, in Figures 6a and b are shown, respectively, the copper reflectivity at different grazing angle θ and He transmission (for distance = 0.5 cm and p = 1 atm) (*4*). We note that optimal grazing angle for stopping the X-ray greater than ≈900 eV is $\theta = 5°$ and the He absorbs at energy lower than ≈200 eV realizing a partial

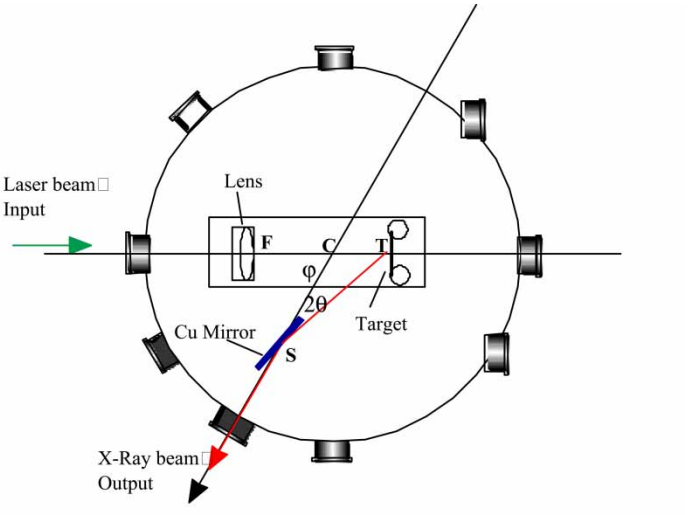

Geometrical relation:

$$l = h\ \sin(\varphi - 2\theta)/\sin(2\theta).$$

l = CS (distance of the chamber centre – Cu mirror centre)
h = CT (distance of the chamber centre – Target position)

S = Cu mirror centre	φ angle = FCS
C = Chamber centre	θ angle = grazing angle to surface of the Cu mirror
T = Target position	2θ angle = CST

Figure 5. The geometrical relation from φ angle (formed by laser beam direction and X-ray beam direction), θ angle (grazing angle to the surface of the mirror or the crystal), l (CS distance in figure) and h (CT distance in figure) are shown.

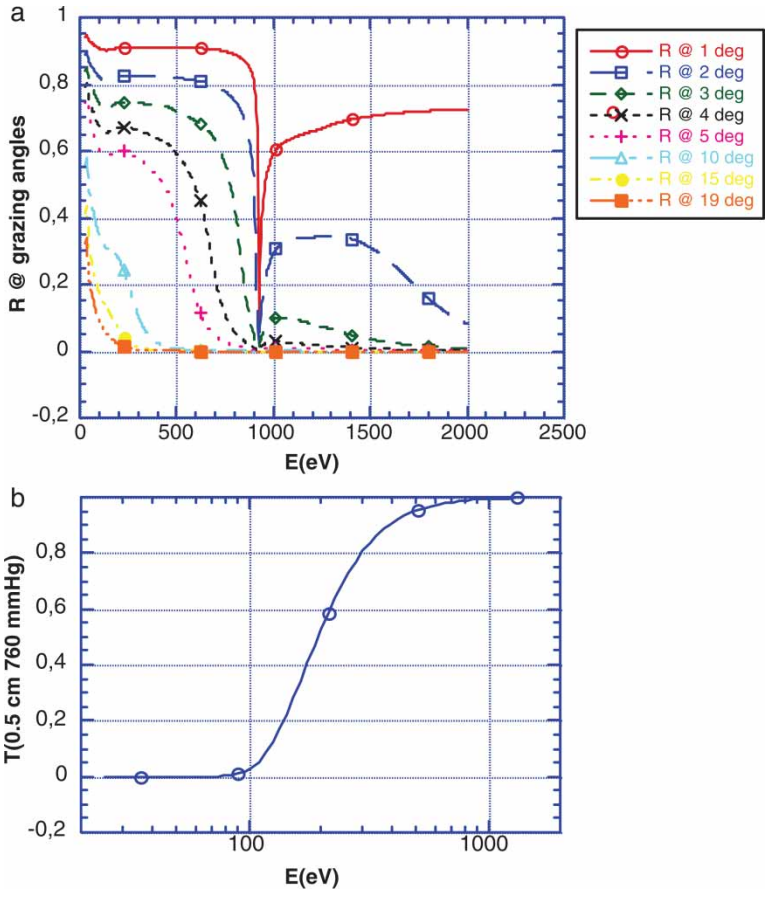

Figure 6. (a) The curves of the copper reflectivity at different grazing angles θ. We note that for $\theta = 5$ degree the X-rays with energy greater ≈900 eV are absorbed and the reflectivity is about 50%. (b) The curve of He transmission (for distance = 0.5 cm and p = 1 atm) is shown. We note that the He absorbs at energy lower than ≈200 eV.

monochromatic beam at large band. The X-ray in energy and intensity will be measured by PIN (Positive-Intrinsic-Negative) diode solid state detector filtered with microfoils of different thickness (about 1 μm or submicrons) and materials and by spectrometers based on KAP (potassium hydrogen phthalate) crystals or mica crystals, respectively.

The X-ray of the higher energy region (about 25 keV) are produced for bremmsthralung effect; the external electrical field is very efficient only for a Debye radius r_D because, as in this case, for long laser pulse duration the plasma reaches the local thermodynamic equilibrium (LTE) condition (*5*). While the non-LTE conditions are present only in the first hundreds of picoseconds of the laser pulse duration with plasma density close to solid density (*6*).

r_D, the characteristic distance at which the plasma screens the external field, is defined as

$$r_D = \left[\frac{kT}{(4\pi ne^2)}\right]^{1/2} = 7.43 \times 10^2\, T^{1/2}\, n^{-1/2}\,\text{cm}$$

where T is the plasma temperature in electron volts and n the electron density in cm^{-3}. Usually, only the electrons localized in the Debye radius are not in equilibrium with the plasma and sensitive to accelerating external fields (*7*). Then, the plasma can be considered as an electron source and the current of the electron beam extract from plasma cathode is, in first approximation, independent

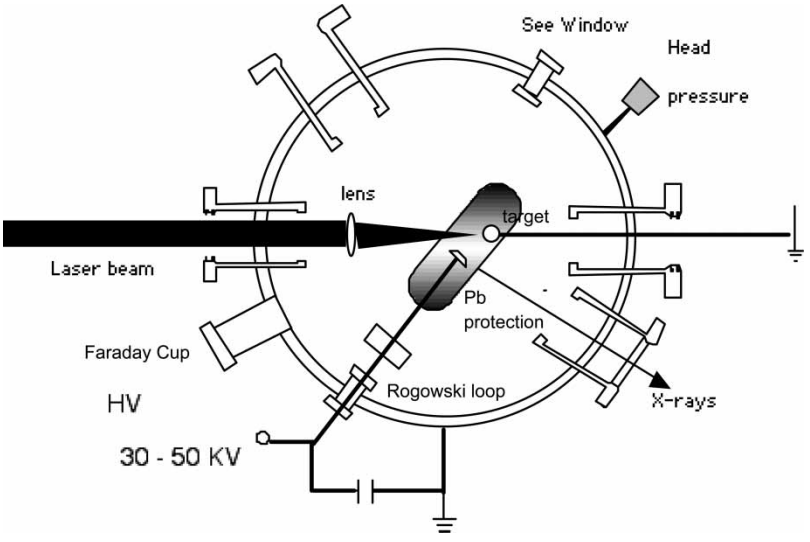

Figure 7. Configuration of the interaction chamber as hard X-ray source (configuration 2). The work pressure is $p = 10^{-7}$ Torr.

of the intensity of the electrical field. So, the X-ray energy can be modulated independently from the X-ray intensity. The X-ray energy depends on the High Tension (HT) voltage and the X-ray intensity is related to the plasma conditions such as the plasma temperature and the ionization degree. Referring to the over-described experimental set-up, the power density focalized on the target ($\approx$80 μm diameter) ranges from 10^{12} to 10^{14} W/cm^2 corresponding to laser energy interval of 250 mJ–8 J (at 1064 nm) and a plasma temperature of about 100 eV.

The relative configuration of the interaction chamber (configuration 2) is shown in Figure 7. With respect to the configuration 1 (Figure 4a), the main difference is the application of the HT voltage (30–50 kV) from the target on which the laser is focalized (cathode) and the anode (such as metallic materials Mo or W) where X-rays are produced for bremmsthralung effect. A Faraday cup and a Rogowsky loop are used to measure the ionization state of the plasma and the intensity of the electronic current.

3. Conclusions

The characteristics of a Nd:YAG/glass high-power laser and the preliminary power density on a copper target are measured. The power density is about 10^{12} W/cm^2. More accurate measurements of the focal spot dimensions will be executed using a pinhole camera. A new mobile disposition of the target–laser system and the mirror/crystal holder put inside the interaction chamber have been illustrated.

In this research, the physical relations from the plasma parameters and the X-ray emission are studied. An important goal of this apparatus is the realization of a system for applications in biomedical field; the possibility of the use of plasma as electron source instead of the hot filament in medical X-ray tubes is investigated, in particular, for mammographic imaging.

Acknowledgements

We would like to thank Prof. E. Coccia Director of Gran Sasso National Laboratories of INFN and Prof. S. Santucci Director of Physics Department of L'Aquila University for supporting us. This work is financially supported by INFN, LASEX experiment.

References

(1) Limongi, T.; Palladino, L.; Bernieri, E.; Tomassetti, G.; Reale, L.; Flora, F.; Cesare, P.; Ercole, C.; Aimola, P.; Ragnelli, A.M. *J. Phys. IV France* **2003,** *104,* 345–348.
(2) Turcu, I.C.E.; Tallents, G.J.; Ross, I.N.; Michette, A.G.; Schultz, M.S.; Meldrum, R.A.; Wharton, C.W.; Batani, D.; Martinetti, M.; Mauri, A. *Phys. Med.* July–September, **1994,** *X* (3), 93–99.
(3) Mallozzi, P.J.; Epstein, H.M.; Jung, R.G.; Applebaum, D.C.; Fairand, B.P. and Gallagher, W.J. *J. Appl. Phys.* **1974,** *45* (4), 1891–1895.
(4) Calculated from *X-Ray Data Booklet*. Center for X-ray Optics and Advanced Light Source, Compiled and edited by Albert C. Thompson and Douglas Vaughan, Lawrence Berkeley National Laboratory – University of California, Berkeley, California 94720, 2001.
(5) O'Neill, F. *Laser Plasma XUV Source*, RAL Report, RAL-88-101, November 1988.
(6) Alaterre, P.; Pépin, H.; Fabbro, R.; Faral, B. *Phys. Rev. A* **1986,** *34* (5), 4184–4194.
(7) Smirnov, B.M. *Introduction to Plasma Physics;* Mir Publishers: Moscow, 1977.